Received January 29, 2018, accepted March 1, 2018, date of publication March 13, 2018, date of current version April 18, 2018.
Digital Object Identifier 10.1109/ACCESS.2018.2813299

Optimum Design of Low-Cost Dual-Mode Beam-Steerable Arrays for Customer-Premises Equipment Applications

WAN WAN[1], WEN GEYI[1], (Member, IEEE), AND STEVEN GAO[2], (Senior Member, IEEE)
[1]Nanjing University of Information Science and Technology, Nanjing 210044, China
[2]School of Engineering and Digital Arts, University of Kent, Canterbury, CT2 7NT, U.K.
Corresponding author: Wan Wan (wanwan92217@163.com)

ABSTRACT Two novel designs of dual-mode beam-steerable array antennas are proposed for customer-premises equipment applications. To obtain the optimal distribution of excitations for the arrays, the gain and front-back ratio of the array systems are optimized by using the method of maximum power transmission efficiency. The first design operates at 2.45 GHz and uses four folded monopoles of height <1/10 wavelength and a sleeve of height of 1/4 wavelength underneath the monopoles. The peak gain and the front-to-back ratio are 6.7 dBi and 7.8 dB respectively. The second design operates at 830MHz and uses four Yagi monopoles as elements with a common reflector and four directors. The peak gain and the front-to-back ratio for the second design are 6.0 dBi and 16.8 dB respectively. The proposed antennas have advantages including: low cost and compact size; dual-mode operation including the modes of omnidirectional radiation and directional radiation; and in the mode of directional radiation, the beam can be electronically steered to achieve the full coverage of the azimuthal plane. It achieves higher gain than the traditional electronically steerable passive array radiator antenna.

INDEX TERMS Antenna gain, beamforming, folded monopole, Yagi antenna, customer-premises equipment.

I. INTRODUCTION

Customer-premises equipment (CPE) refers to an equipment located at a subscriber's premises and connected with a carrier's telecommunication channel. In many situations, the CPE must be "smart" enough to be able to steer the radiation pattern towards the desired direction for enhancing the performance of wireless communications. Smart antenna with two radiation modes for CPE applications [1]–[7] must have compact size, low cost and require the beam steering in the azimuth plane. One mode is the omni-directional radiation mode with omni-directional coverage in the azimuth plane to search for the transmitting source while the other mode is the directional radiation mode to communicate with high gain and high data-rate. Due to the cost reduction requirement, a compromise must be made between the complexity and performance of the CPE system. A simple approach to the CPE antenna design is to use reactively loaded array or electronically steerable passive array radiator (ESPAR) [8]–[11]. Recently, a new single-anchor indoor localization concept employing ESPAR antenna with a simple fingerprinting algorithm has been proposed in [12].

Several examples of ESPAR antenna have been studied in [13]–[17]. In an ESPAR array, only one driven element is connected to the RF port while other elements are parasitic elements with reactive or resistive loads which can be electronically controlled by changing the DC voltages of the varactors, etc. To obtain the optimum values of loaded varactors, the modal-expansion method has been used for analyzing ESPAR driven by a small gap source [13]. In order to replace the method of applying correct bias voltages to varactor diodes, the ESPAR antenna with simplified beam-steering circuit, which relies on RF switches providing required load to the parasitic elements has been proposed in [14]. Most methods focus on reducing the capacitive loading introduced by parasitic elements. One method is to increase the length of the parasitic monopoles to achieve impedance matching [15], however, the size of antenna is increased. The size reduction of smart antenna is a key requirement for CPE applications. To further reduce the size of ESPAR antenna, the dielectric embedded ESPAR antenna (DE-ESPAR) with new embedded dielectric material was presented [16]. An overall volume reduction of 80% and a maximum gain of 5.1 dBi were achieved in the seven-element DE-ESPAR antenna. A compact ESPAR using inverted-F antenna elements was reported in [17]. The radius of ESPAR antenna can be reduced by using the capacitive coupling between antenna elements, as shown in [19]. It achieves a gain of 4.0 dBi and a front-back ratio of 20 dB.

The major advantage of the ESPAR antenna is the capability of realizing beam scanning without using a complicated beamforming network as in phased arrays. However, the ESPAR antenna beam scanning requires considerable data processing with regard to the excitation inputs related to the direction-of-arrival (DOA). Due to the limited range of phase changes of antenna elements, one cannot guarantee the best possible gain performance for an ESPAR antenna. In addition, the design of electrically small antenna arrays with a relatively high gain and practically useful bandwidth represents a more challenging task for CPE applications. Furthermore, the low cost phase shifters and attenuators chips are available in some RF and microwave frequency bands nowadays so that a feeding circuit can be easily built. For the above reasons, it is worth exploring the possibility of maximizing the CPE antenna gain while the antenna size is held small.

In this paper we will apply the power transmission formula between two antenna arrays [20], [21] to the design of typical CPE antennas to explore the possibility of achieving maximum possible antenna gain for a fixed geometry. Two novel designs will be investigated to demonstrate the advantages of the method. Our first design is a four-element folded monopole array antenna operating at 2.45 GHz, in which the height of the elements is less than wavelength/10 with a copper sleeve as ground. The four-element folded monopole array is capable of beam scanning in the horizontal plane and has a directional gain of 6.7 dBi, which is 2.7dB higher than the seven-element ESPAR antenna of similar type in [19]. Our second design operates at 830MHz and makes use of four identical Yagi monopoles as elements with a common reflector and ground plane. The peak gain and the front-to-back ratio are 6.0 dBi and 16.8 dB respectively.

II. DESIGN METHOD

To achieve the optimized design of the antenna arrays proposed, a brief introduction of the optimization theory is given below. The antenna system consists of N-elements and a testing antenna is introduced so that the whole system may be considered as one network with (N + 1) ports, as shown in Fig. 1. The power transmission efficiency T between the transmitting antenna array and the test receiving antenna is defined as the ratio of the power delivered to the load of the test receiving antenna to the input power to the transmitting antenna array

$$T = \frac{\frac{1}{2}(|[b_r]|^2 - |[a_r]|^2)}{\frac{1}{2}(|[a_t]|^2 - |[b_t]|^2)} \tag{1}$$

where

$$[a_t] = [a_1, a_2, \ldots, a_N]^T,$$
$$[a_r] = [a_{N+1}],$$
$$[b_t] = [b_1, b_2, \ldots, b_N]^T,$$
$$[b_r] = [b_{N+1}],$$

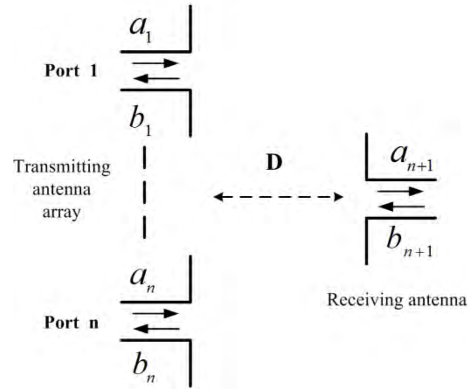

FIGURE 1. Power transmission between transmitting antenna array and receiving antenna.

denote incident and reflected waves for the transmitting. Assuming that the receiving antenna is well-matched and the power transmission efficiency reaches the maximum, equation (1) reduced to

$$[A][a_t] = T[a_t] \tag{2}$$

where $[A] = [\bar{S}_{rt}]^T S_{rt}$, and S_{rt} represent the scattering parameters for the transmission system and can be obtained by simulation tools such as ANSYS HFSS(High Frequency Structural Simulator) or by measurements. Once the S-parameter matrix is known, the optimum excitation distribution for the transmitting antenna array can be obtained by solving the eigenvalue problem of equation (2). The unique nontrivial eigenvalue of the above equation gives the maximum power transmission efficiency, and the corresponding eigenvector is the optimal excitation distribution for the transmitting antenna array. The details of the optimization theory are given in [20] and [21].

The above method is versatile in the antenna array design and has been successfully applied in the designs of focused antennas [22], smart antennas [23], and wireless power transmission (WPT) systems [24]. To further investigate the applicability of the method, antenna designs in unknown electromagnetic environments were proposed in [25]. Note that the effects of the mutual coupling between the transmitting antenna elements and the environments have been included in the scattering matrix.

III. ANTENNA DESIGNS AND RESULTS

A. DESIGN1: FOLDED MONOPOLE ANTENNA ARRAY

The smart arrays using monopole antennas have been studied in [8]–[12] and [19]. To reduce the height, a folded monopole may be used as the antenna element [19], [26]. A four-element folded monopole antenna array has been designed by using (2). Fig. 2 (a) and 2 (b) show the side view and top view of the antenna designed, while a photo of the fabricated antenna is given in Fig.2 (c). The folded monopole and the sleeve ground form a quasi-balanced radiating structure. The short monopole and its image in the sleeve ground may be

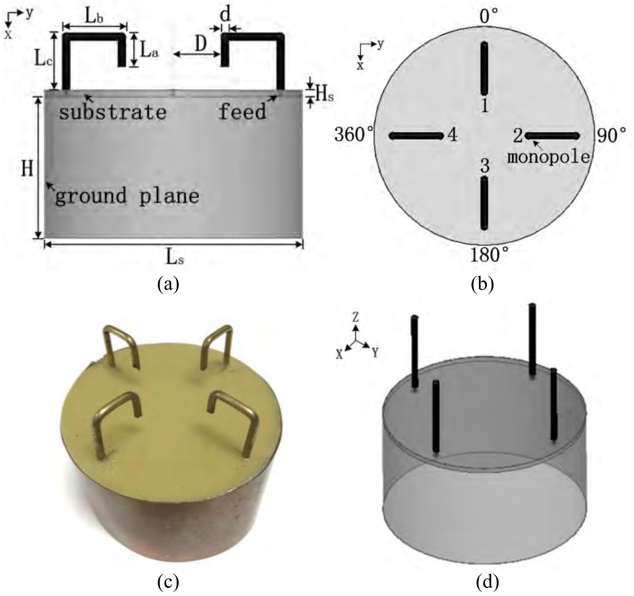

FIGURE 2. The configuration of the fold monopole antenna array operating at 2.45 GHz. (a) Side view. (b) Top view. (c) Photo. (d) The straight monopole antenna array configuration.

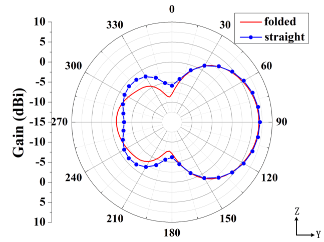

FIGURE 3. Simulated radiation patterns of the folded monopole antenna array and the straight monopole antenna array with a sleeve ground in the xy-plane.

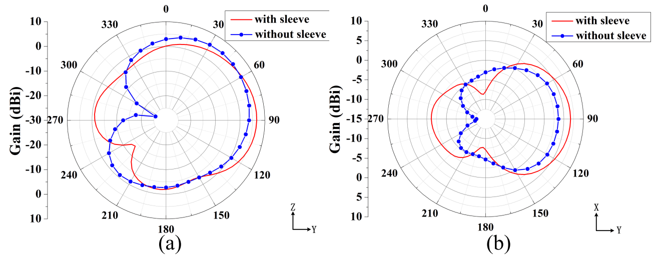

FIGURE 4. Simulated radiation patterns of the folded monopole antenna array with and without a sleeve ground plane (a) yz-plane (b) xy-plane.

considered as a short dipole so that the radiation pattern in the horizontal plane has good omnidirectional performance. Each folded monopole is connected to one of the ports of a beamforming network. The total radiation pattern is determined by the surface currents on all radiating elements. The surface currents can be controlled by varying the voltages applied to attenuators and phase shifters in the beamforming network. The symmetrical arrangement of the four-element array enables the radiation pattern to sweep in the horizontal plane with a minimum gain variation. The optimized parameters of the proposed antenna array are listed in Table 1.

TABLE 1. Parameters of monopole array.

Parameter(mm)	value
L_a	7
L_b	13
L_c	10.8
D	12
H_s	1.6
L_s	60
H	30
d	2

To see the influence of folded monopole on the radiation pattern, a comparison is made between the folded and straight monopole array with same sleeve ground, and is shown in Fig. 2. The results are based on the same antenna sizes (length and radius) with one monopole being folded and the other being straight. The folded monopole is reduced in height by 60% compared to a straight monopole antenna while the gain decreases only 0.2dBi as indicated by Fig. 3. The sleeve ground with a height of one-quarter wavelength is used to tune the direction of maximum radiation to horizontal plane [18], [19]. In order to see this effect, the simulated radiation patterns in yz-plane and xy-plane for the folded monopole arrays with and without sleeve ground are given in Fig. 4 (a) and (b). It is clearly shown in Fig. 4 that the direction of the maximum gain of the array without sleeve ground is 30 degrees off the Z axis. For the folded monopole array with the sleeve ground, the maximum gain direction is tuned to the horizontal plane. Its gain reaches 6.7 dBi, which is 3.1dB higher than that of no sleeve ground.

ESPAR antennas with reactive or resistive loads can ease the work of designing a feeding network. The phase tuning can be achieved by adjusting the control voltages applied to the varactors. However, the main disadvantages of the ESPAR antennas are the considerable digital processing and nonlinearity. To simplify the digital processing and guarantee that the smart antenna can achieve 360° beam scanning in horizontal plane with higher gain, a beamforming network for the array is also designed and implemented.

Fig. 5 (a) and (b) show the schematic and the photo of the four-port beamforming network. As shown in Fig. 5, four low-cost phase shifters are employed. In this design, the phase shifter is used to change the phase and the amplitude is controlled by the attenuator, and a power splitter is used to keep the isolations among the four ports below −20 dB. The voltage regulator circuit plays an important role in the beamforming network, and controls the outputs of the attenuators and phase shifters.

By adjusting the rheostat on the beamforming network to control the attenuator and the phase shifter, the antenna array can achieve the optimized distribution of amplitudes and phases. When the input voltage is 9V, the output voltages of the attenuator range from 0 to 9V, while the output voltages

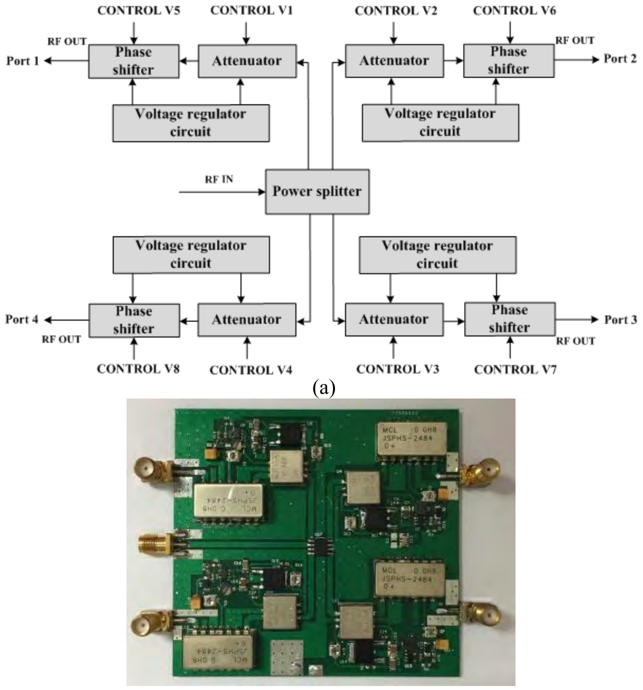

FIGURE 5. The design of the beamforming network. (a) Schematic. (b) Photo.

of the phase shifter range from 2.5 to 15 V. The Ohm losses of the beamforming network are 0.8dB, 0.3dB and 0.5dB in the state of 0°, 30° and 45° respectively. The loss has been taken into account while measuring the gain and bandwidth for different beamforming states.

The four-element folded monopole array is connected to the beamforming network and is fabricated on a FR4 substrate. The measured and simulated reflection coefficients are given in Fig. 6. It can be seen that the bandwidth of the four-element folded monopole array ranges from 2.27 to 2.75 GHz. When the amplitudes and phases at the four feeding ports are uniform, the radiation pattern becomes omni-directional in the xy-plane, and is symmetrical in the yz-plane as shown in Fig. 7. The measured gain for the omni-directional pattern is 1.7 dBi in the xy-plane.

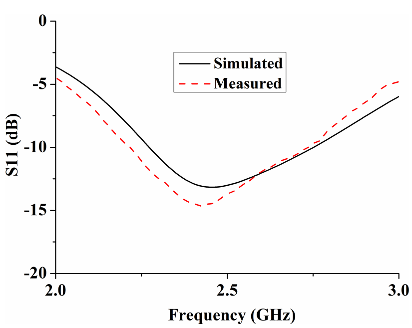

FIGURE 6. Reflection coefficients of the folded monopole array.

Table 2 shows the optimized excitation distributions obtained by solving (2) for various steering angles in

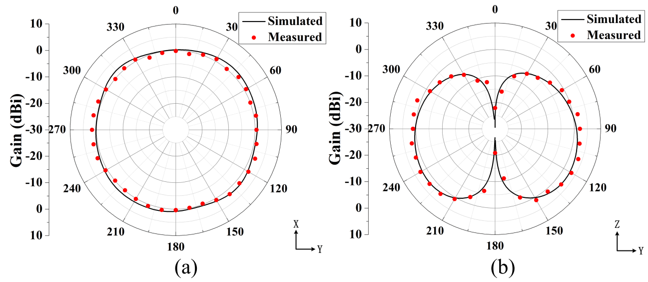

FIGURE 7. Omni-directional radiation patterns of folded monopole antenna array at 2.45 GHz (a) xy-plane,(b) yz-plane.

TABLE 2. Distribution of excitations.

Angle	Port 1	Port 2	Port 3	Port 4
0°	0.73∠-78	0.39∠0	0.41∠103	0.39∠0
30°	0.67∠0	0.51∠25	0.41∠162	0.35∠124
45°	0.60∠0	0.60∠0	0.38∠137	0.38∠137
60°	0.52∠0	0.66∠-27	0.35∠100	0.41∠135
90°	0.39∠0	0.73∠-78	0.39∠0	0.41∠103
180°	0.41∠103	0.39∠0	0.73∠-78	0.39∠0
270°	0.39∠0	0.41∠103	0.39∠0	0.73∠-78

directional radiation mode. The radiation pattern steered at 0°, 90°, 180°, and 270° are shown in Fig. 8 while those steered at 30°, 45° and 60° in Fig. 9. Compared with omni-directional transmission, the gain from the beamforming has been increased significantly. As indicated in Fig. 9, the measured gain of the four-element antenna array with the optim ized excitations from (2) is 6.7dBi, which is 0.7dBi higher than the similar design of fourteen-element ESPAR antenna array in [26].

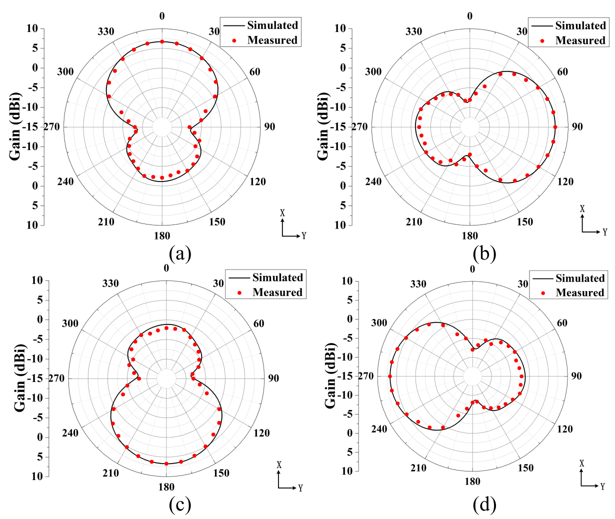

FIGURE 8. Radiation patterns of folded monopole antenna array at 2.45 GHz steered at (a) 0° (b) 90° (c) 180° (d) 270°.

B. DESIGN2: MONOPOLE YAGI ANTENNA ARRAY

Our first design investigated in section A is suitable for the situation where the diameter of the cylindrical structure is required to be small. In order to tune the radiation pattern to the horizontal plane, the height of the sleeve ground must

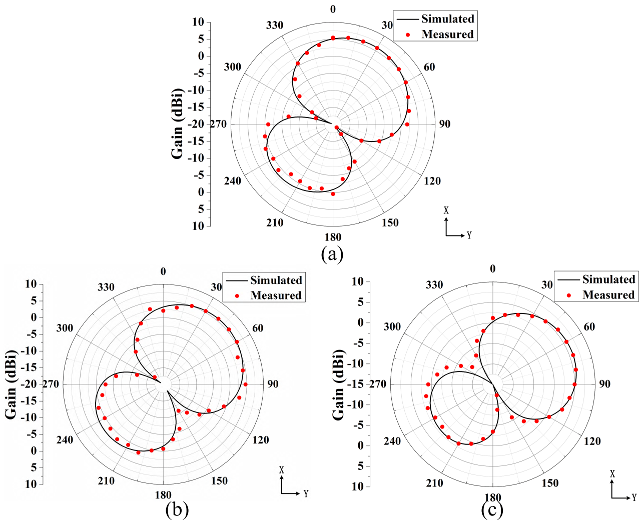

FIGURE 9. Radiation patterns of folded monopole steered at (a) 30 (b) 45° (c) 60°.

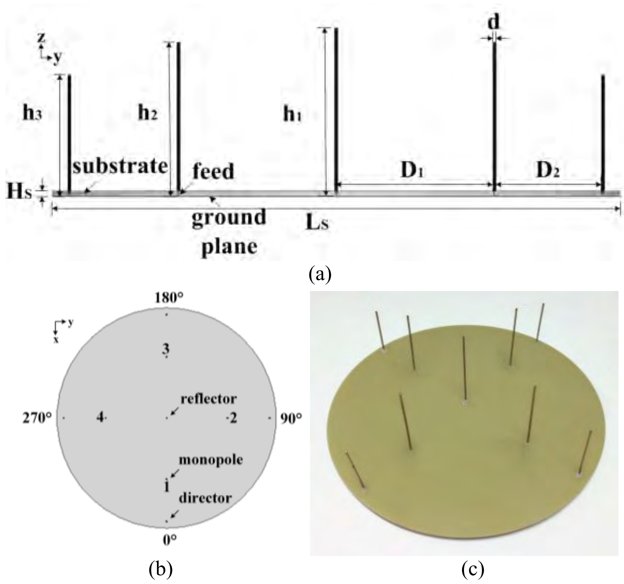

FIGURE 10. The configuration of Yagi monopole antenna array operating at 830 MHz. (a) Side view. (b) Top view. (c) Photo.

be one-quarter wavelength, which may be too long for some low frequency applications. In this section, we demonstrate a second CPE antenna design which operates at 830MHz. A new arrangement of monopole antennas without using the sleeve ground to tune the direction of maximum radiation into horizontal plane is proposed. To realize omni-directional scanning and achieve higher front-to-back ratio, four Yagi monopole sub-arrays with one common reflector are introduced. Fig. 10 (a) and (b) show the side view and top view of the antenna designed, while a photo of the fabricated antenna is given in Fig 10 (c). The size optimization of the director element and the reflector element has been taken into consideration in the whole design process as was done in [27]. The optimized parameters of the Yagi monopole antenna array are listed in Table 3. The height of the Yagi antenna has been reduced when comparing to the antenna mentioned in design 1, however, its diameter is larger.

TABLE 3. Parameters of monopole array.

Parameter(mm)	value
L_s	324
H_s	3
h_1	96
h_2	88
h_3	60
D_1	88
D_2	60
d	2

As shown in Fig. 11, the measured reflection coefficient of the Yagi monopole antenna array are below −10dB from 783 to 886 MHz. The beam forming network discussed in section A is applied to realize the optimized amplitudes and phases calculated by the method of maximum power transmission efficiency. The simulated and measured results for the omni-directional radiation patterns (when the array is excited by the uniform amplitudes and phases) are shown in Fig.12. The measured gain is −1.8dBi in the xy-plane in the omni-directional radiation mode. For the directional radiation mode, the optimal distribution of excitations can be obtained by solving (2) and some typical results for different steering angles are listed in Table 4. The radiation patterns steered at 0°, 90°, 180°, 270° are shown in Fig. 13 while those steered at 30°, 45° and 60° in Fig. 14. It can be seen that the horizontal gain can be enhanced to 6.0 dBi while the front-back ratio to 16.8dB.

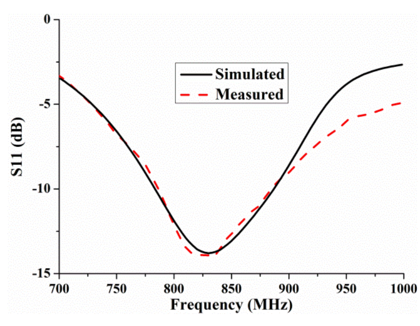

FIGURE 11. Reflection coefficients of Yagi monopole array.

TABLE 4. Distribution of excitations.

Angle	Port 1	Port 2	Port 3	Port 4
0°	0.65∠104	0.45∠0	0.42∠89	0.45∠0
30°	0.60∠0	0.48∠35	0.44∠173	0.46∠138
45°	0.53∠0	0.53∠0	0.45∠144	0.45∠144
60°	0.50∠0	0.62∠-38	0.43∠103	0.43∠137
90°	0.45∠0	0.65∠104	0.45∠0	0.42∠89
180°	0.42∠89	0.45∠0	0.65∠104	0.45∠0
270°	0.45∠0	0.42∠89	0.45∠0	0.65∠104

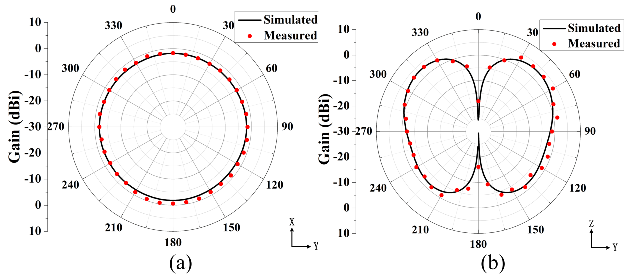

FIGURE 12. Radiation patterns of Yagi monopole array (a) xy-plane (b) yz-plane.

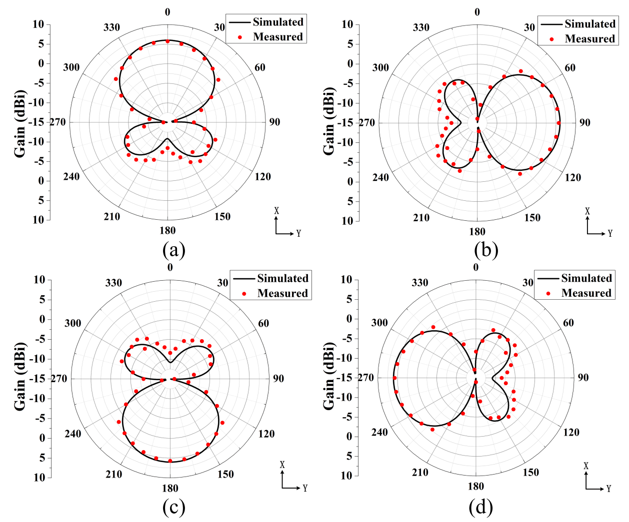

FIGURE 13. Radiation patterns of Yagi monopole array steered at (a) 0° (b) 90° (c) 180° (d) 270°.

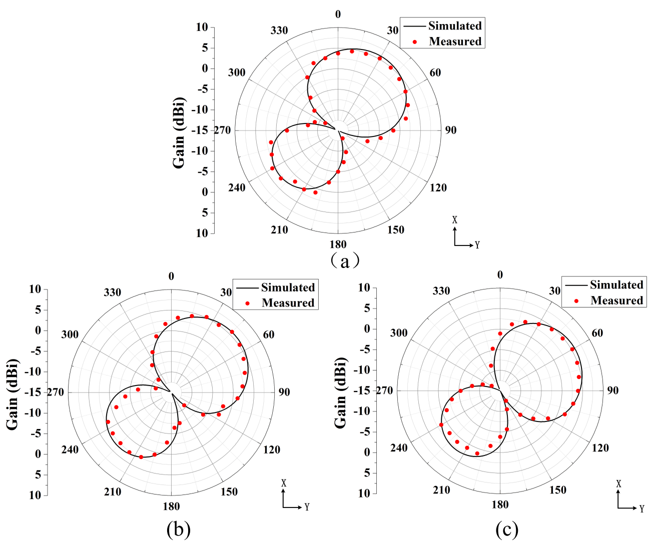

FIGURE 14. Radiation patterns of Yagi monopole array steered at (a) 30° (b) 45° (c) 60°.

To demonstrate the effectiveness of our design method, the performance comparisons of our designs with other similar designs are shown in Table 5. Compared to the antenna array in [19], the proposed array antenna 1 has about the same height but fewer elements while its directional gain is 2.7dB higher. Compared to the ESPAR antenna array in [26], the antenna 1 has smaller height and much fewer elements but higher gain. Also note that the proposed array antenna 2 has smaller relative height and fewer elements comparing to the ESPAR antenna in [26].

TABLE 5. Performance comparison of antennas.

Antenna	Center frequency	Dual mode	Element number	Antenna height	Antenna diameter	Gain
[19]	2.45GHz	No	7	0.35λ	0.5λ	4.0
[26]	2.45GHz	No	14	0.44λ	0.5λ	6.0
Proposed design1	2.45GHz	Yes	4	0.35λ	0.5λ	6.7
Proposed design2	830MHz	Yes	9	0.28λ	0.9λ	6.0

IV. CONCLUSION

Two novel designs of array antennas operating at 2.45 GHz and 830 MHz for CPE applications have been investigated in this paper. The design uses the method of maximization of power transmission efficiency to determine the optimal distribution of excitations. A beamforming network is designed and implemented. For the four-element folded monopole array operating at 2.45GHz, the measured peak gain is 6.7 dBi in the directional radiation mode and 1.7dBi in the omni-directional radiation mode. For the monopole Yagi array operating 830MHz the peak gain is 6.0 dBi in the directional radiation mode and −1.8dBi in the omni-directional radiation mode. In both cases, our design method ensures that the best possible gain performance can be achieved for fixed configuration while the array size is kept small.

REFERENCES

[1] K. Sheikh, D. Gesbert, D. Gore, and A. Paulraj, "Smart antennas for broadband wireless access networks," *IEEE Commun. Mag.*, vol. 37, no. 11, pp. 100–105, Nov. 1999.
[2] H. Bolcskel, A. J. Paulraj, K. V. S. Hari, R. U. Nabar, and W. W. Lu, "Fixed broadband wireless access: State of the art, challenges, and future directions," *IEEE Commun. Mag.*, vol. 39, no. 1, pp. 100–108, Jan. 2001.
[3] C. Oestges, V. Erceg, and A. J. Paulraj, "A physical scattering model for MIMO macrocellular broadband wireless channels," *IEEE J. Sel. Areas Commun.*, vol. 21, no. 5, pp. 721–729, Jun. 2003.
[4] K. M. Nasr, F. Costen, and S. K. Barton, "A wall imperfection channel model for signal level prediction and its impact on smart antenna systems for indoor infrastructure WLAN," *IEEE Trans. Antennas Propag.*, vol. 53, no. 11, pp. 3767–3775, Nov. 2005.
[5] M. I. Lai, T. Y. Wu, J. C. Hsieh, C. H. Wang, and S. K. Jeng, "Compact switched-beam antenna employing a four-element slot antenna array for digital home applications," *IEEE Trans. Antennas Propag.*, vol. 56, no. 9, pp. 2929–2936, Sep. 2008.
[6] Z. Chen and C. Parini, "Low cost shaped beam synthesis for semi-smart base station antennas," *IET Microw., Antennas Propag.*, vol. 10, no. 1, pp. 119–128, Sep. 2015.
[7] M. I. M. Elamin and T. A. Rahman, "2-element slot meander patch antenna system for LTE-WLAN customer premise equipment," in *Proc. IEEE-APS Topical Conf. Antennas Propag. Wireless Commun. (APWC)*, Sep. 2015, pp. 993–996.

[8] R. F. Harrington, "Reactively controlled directive arrays," *IEEE Trans. Antennas Propag.*, vol. 26, no. 3, pp. 390–395, May 1978.
[9] C. Sun, A. Hirata, T. Ohira, and N. C. Karmakar, "Fast beamforming of electronically steerable parasitic array radiator antennas: Theory and experiment," *IEEE Trans. Antennas Propag.*, vol. 52, no. 7, pp. 1819–1832, Jul. 2004.
[10] C. Sun and N. C. Karmakar, "Adaptive beamforming of ESPAR antenna based on simultaneous perturbation stochastic approximation theory," in *Proc. Asia–Pacific Microw. Conf.*, vol. 1. Kyoto, Japan, Nov. 2002, pp. 192–195.
[11] M. Carras, A. Kalis, and A. G. Constantinides, "Improving the frequency characteristics of the electronically steerable passive array radiator antenna," in *Proc. 1st Int. Symp. Wireless Commun. Syst.*, Sep. 2004, pp. 130–134.
[12] M. Rzymowski, P. Woznica, and L. Kulas, "Single-anchor indoor localization using ESPAR antenna," *IEEE Antennas Wireless Propag. Lett.*, vol. 15, pp. 1183–1186, 2016.
[13] Q. Wang and Z. Shen, "Modal-expansion analysis of electrically steerable passive array radiators (ESPAR)," in *Proc. IEEE Antennas Propag. Soc. Int. Symp.*, vol. 4B. Jul. 2005, pp. 27–30.
[14] L. Kulas, "Direction-of-arrival estimation using an ESPAR antenna with simplified beam-steering," in *Proc. 47th Eur. Microw. Conf.*, Nuremberg, Germany, 2017, pp. 296–299.
[15] T. D. Dimousios, C. I. Tsitouri, S. C. Panagiotou, and C. N. Capsalis, "Design and optimization of a multipurpose tri-band Electronically Steerable Passive Array Radiator (ESPAR) antenna with steerable-beam-pattern for maximum directionality at the frequencies of 1.8, 1.9 and 2.4 GHz with the aid of genetic algorithms," in *Proc. LAPC*, Mar. 2008, pp. 253–256.
[16] J. Lu, D. Ireland, and R. Schlub, "Dielectric embedded ESPAR (DE-ESPAR) antenna array for wireless communications," *IEEE Trans. Antennas Propag.*, vol. 53, no. 8, pp. 2437–2443, Aug. 2005.
[17] H. Liu, S. Gao, and T. H. Loh, "Small smart antenna composed of reconfigurable inverted F-type antenna," in *Proc. Int. Conf. Microw. Technol. Comput. Electromagn. (ICMTCE)*, Nov. 2009, pp. 33–36.
[18] H. Kawakami and T. Ohira, "Electrically steerable passive array radiator (ESPAR) antennas," *IEEE Antennas Propag. Mag.*, vol. 47, no. 2, pp. 43–50, Apr. 2005.
[19] H.-T. Liu, S. Gao, and T.-H. Loh, "Electrically small and low cost smart antenna for wireless communication," *IEEE Trans. Antennas Propag.*, vol. 60, no. 3, pp. 1540–1549, Mar. 2012.
[20] W. Geyi, *Foundations of Applied Electrodynamics*. New York, NY, USA: Wiley, 2010, pp. 273–275.
[21] W. Geyi, *Foundations for Radio Frequency Engineering*. Singapore: World Scientific, 2015, pp. 410–420.
[22] L. Shan and W. Geyi, "Optimal design of focused antenna arrays," *IEEE Trans. Antennas Propag.*, vol. 62, no. 11, pp. 5565–5571, Nov. 2014.
[23] H. P. Tong and W. Geyi, "Optimal design of smart antenna systems for handheld devices," *IET Microw., Antennas Propag.*, vol. 10, no. 6, pp. 617–623, Jun. 2016.
[24] X. Yang, W. Geyi, and H. Sun, "Optimum design of wireless power transmission system using microstrip patch antenna arrays," *IEEE Antennas Wireless Propag. Lett.*, vol. 16, pp. 1824–1827, 2017.
[25] H. Sun and W. Geyi, "Optimum design of wireless power transmission systems in unknown electromagnetic environments," *IEEE Access*, vol. 5, pp. 20198–20206, 2017.
[26] H. Liu, S. Gao, and T. H. Loh, "Compact MIMO antenna with frequency reconfigurability and adaptive radiation patterns," *IEEE Wireless Antenna Propag. Lett.*, vol. 12, pp. 269–272, 2013.
[27] C. Phongcharoenpanich, C. Buranakunaporn, and S. Kosulvit, "Characteristics of monopole Yagi array antenna on the ground plane with direction of arrival estimation," in *Proc. 9th Asia–Pacific Conf. Commun.*, vol. 3. Sep. 2003, pp. 969–973.

WAN WAN was born in Jiangsu, China, in 1992. She received the M.Eng. degree in electrical engineering from the Nanjing University of Information Science and Technology, Jiangsu, China, in 2015. Her research interests include antenna arrays and beamforming network.

WEN GEYI (M'88) was born in Hunan, China, in 1963. He received the B.Eng., M.Eng., and Ph.D. degrees in electrical engineering from Xidian University (formerly Northwest Telecommunications Institute), China, in 1982, 1984, and 1987 respectively.

He was a Lecturer with the Radio Engineering Department, Southeast University, from 1988 to 1990; an Associate Professor with the Institute of Applied Physics, University of Electronic Science and Technology of China (UESTC), from 1990 to 1992; a Visiting Researcher with the Department of Electrical and Computer Engineering, University of California at Berkeley, from 1992 to 1993; a Full Professor with the Institute of Applied Physics, UESTC, from 1993 to 1998; a Visiting Professor with the Electrical Engineering Department, University of Waterloo, in 1998. From 1996 to 1997, he was the Vice Chairman of the Institute of Applied Physics, UESTC, and also the Chairman of the Institute from 1997 to 1998. From 1998 to 2007, he was with Research In Motion Ltd. (now Blackberry Ltd.), Canada, first as a Senior Scientist with the Radio Frequency Department and then the Director of the Advanced Technology Department. Since 2010, he has been the National Distinguished Professor of China, first with Fudan University, Shanghai, and then with the Nanjing University of Information Science and Technology (NUIST), Nanjing, China. He is currently the Director of the Research Center of Applied Electromagnetics, NUIST. His current research interests include microwave theory and techniques, and antennas and wave propagation. He is also the Inventor of over 30 patents and has over 100 publications. He is the author of *Modern Methods for Electromagnetic Computations* (in Chinese, Henan Science and Technology Press, 1994), *Advanced Electromagnetic Field Theory* (in Chinese, National Defense Publishing House, 1999), *Foundations of Applied Electrodynamics* (Wiley, 2010), and *Foundations for Radio Frequency Engineering* (World Scientific, 2015).

STEVEN (SHICHANG) GAO was born in Anhui, China. He received the Ph.D. degree in microwave engineering from Shanghai University, Shanghai, China, in 1999. He was a Senior Lecturer and a Group Leader in antennas and RF systems with the Surrey Space Center, University of Surrey. He is currently a Professor with the School of Engineering and Digital Arts, University of Kent, U.K. His research interests include satellite antennas, smart antennas, RF/microwave/mm-wave circuits, wireless systems, and small satellites.